CMBES/SCGB
2025 CMBEC47/ACCES26
Fredericton, NB
May 27-29, 2025

Automated 3D Doppler Ultrasound Imaging for Comprehensive Breast Lesion Assessment

Amal Aziz[1,5], Rayhan Abdul Rahman[2], Claire K. Park[3], Tiana Trumpour[4,5], Jeffrey Bax[5], Lori Gardi[5], David Tessier[5], Kevin Barker[5], Tamie Poepping[2], Aaron Fenster[1,4,5]

[1]School of Biomedical Engineering, Faculty of Engineering, Western University, London, Canada, [2]Dept. of Physics & Astronomy, Faculty of Science, [3]Division of Medical Physics and Biophysics, Dept. of Radiation Oncology, Brigham and Women's Hospital and Dana-Farber Cancer Institute, Harvard Medical School, Boston, USA, [4]Depart. of Medical Biophysics, Schulich School of Medicine and Dentistry, Western University, [5]Imaging Research Laboratories, Robarts Research Institute, London, Canada

Abstract— **Breast cancer is the most common cancer in women worldwide. There are two million diagnoses and 685,000 deaths annually. Early diagnosis is critical to reducing mortality. Although screening with mammography has been shown to have reduced breast cancer-related mortality through early detection, dense breast tissues reduce mammographic sensitivity, potentially delaying diagnoses and contributing to poorer outcomes. Therefore, there is a need for more accessible and cost-effective supplemental screening technologies, especially for high-risk populations and women with dense breasts. To address these challenges, a promising approach involves combining widely available, cost-effective, and accessible ultrasound-based technologies with economical hardware, software modules, and automated techniques. Among these technologies, Doppler imaging plays a crucial role in the clinical evaluation of breast abnormalities, as intratumoural blood flow has been shown to correlate with the aggressiveness and histological grade of the tumour. The development of a novel automated, portable, and patient-dedicated 3D automated breast ultrasound (ABUS) system for point-of-care breast cancer supplemental screening holds significant promise. The proposed system has previously demonstrated the capability to generate accurate whole-breast B-mode images, which can aid in the early detection of breast cancer in women with dense breasts. Additionally, it offers the advantage of incorporating Doppler imaging to assess blood flow within suspicious lesions, a capability not commonly available with commercial ABUS systems. By leveraging Doppler imaging in conjunction with 3D B-mode ABUS, this innovative approach could improve breast cancer-related health outcomes and equity in access to healthcare, especially for underserved and vulnerable populations.**

Keywords— **automated breast ultrasound, power Doppler, superb microvascular imaging, breast cancer, system development**

I. Introduction

Breast cancer is the most common cancer in women worldwide. There are two million diagnoses each year and 685,000 deaths [1]. Apart from adjuvant therapies, such as chemotherapy or hormone treatment, timely diagnosis is a primary pathway by which breast cancer mortality rate can be reduced [2]. Mammography currently stands as the gold standard in breast cancer screening; however, it has reduced sensitivity in women with dense breasts [3]. Malignancies are more difficult to identify in women with more dense fibroglandular tissue compared to fatty adipose tissue. Additionally, breast density alone is a strong, independent risk factor for developing breast cancer [4]. This has the potential to delay diagnoses, contributing to overall poorer outcomes in populations with dense breasts. Navigating the intricacies involved with screening women with dense breasts may often require additional supplemental imaging, such as magnetic resonance imaging (MRI) and tomosynthesis [5]. However, these procedures are often costly and require experienced technicians, making them inaccessible in limited-resource settings. Therefore, there is a need for the development of accessible, cost-effective, and point-of-care technologies for the early diagnosis of breast cancer, especially in underserved populations and women with dense breasts.

Conventional ultrasound (US) is a non-invasive and widely accessible imaging modality, making it particularly suitable for this application. However, B-mode US images somewhat incompletely convey the severity of tumours. Doppler US, which utilizes the Doppler effect to characterize blood flow, is particularly useful when imaging breast tissue as it can provide information on intratumoural blood flow, which correlates with tumour aggressiveness and histological grade. [6] Furthermore, it can help distinguish between some cysts and anechoic malignant lesions [7]. Specifically, power Doppler (PD) and superb microvascular imaging (SMI) are both techniques that can be used to visualize intratumoural blood flow given their ability to image low-velocity blood flow as well as flow within microvasculature [8], [9], [10].

Our lab has previously designed and constructed a cost-effective, wearable 3D automated breast ultrasound (ABUS) device, as shown in Fig. 1, which can generate whole breast images using any commercially available US system and transducer. Integrating automated 3D whole breast imaging with diagnostic Doppler characterisation

has the potential to facilitate definitive diagnosis of breast cancer in increased-risk populations, especially in women with dense breasts. This work represents the first integration of 3D Doppler imaging with an ABUS system, a capability currently lacking from commercial systems [11]. As such, this paper focuses on the integration and characterization of 3D Doppler imaging within our previously developed 3D ABUS device.

II. METHODS

A. System Description and Software Components

The design and functionality of the 3D ABUS system, including its scanning mechanism and imaging reconstruction, have been described in detail in previous work [12], [13]. We extended our system's capability by modifying image reconstruction and visualization. This included capturing color voxels alongside grayscale voxels, as well as optimizing scanning parameters to minimize presence of artifacts. The system is comprised of a custom 3D-printed wearable base that conforms to patient anatomy, an adjustable compression assembly to stabilize the breast, and a mechanically driven scanning mechanism [14]. While the system can be adapted to any commercial ultrasound system, for testing purposes, a Canon Aplio i700 US system (Canon Medical Systems, Tochigi, Japan) and a high-resolution 14L5 (10 MHz) linear transducer were used. Our imaging system includes a workstation capable of real-time US image acquisition, 3D US reconstruction, multi-planar visualization, and a complementary (CBUS) acquisition approach to improve resolution [15], [16].

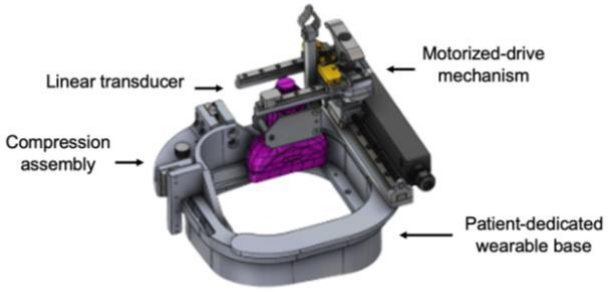

FIG 1. Computer-aided design (CAD) illustrating the 3D ABUS system with the patient-dedicated base and the motorized drive for scanning the US transducer.

B. Phantom Description

The 3D Doppler capabilities of the hardware and software were tested using two custom-designed flow phantoms. The first mimicked a vessel embedded in tissue, which was designed using Fusion360 (Autodesk, San Francisco, CA) and Meshmixer (Autodesk, San Francisco, CA). The vessel mimic was then 3D-printed (Form3BL, Formlabs, Sommerville, MA) using photopolymerization of a proprietary resin (Elastic50A, FormLabs, Sommerville, MA). The model had an overall diameter of 25 mm, a vessel inner diameter of 2 mm, and a vessel wall thickness of 0.65 mm. These parameters were selected for consistency with physiological vessel morphology, as shown in Fig. 2. The printed vessel was embedded in colloidal agar-based background material, consisting of 3% agar by mass. 8% glycerol by mass was added to provide the phantom's speed-of-sound to be the same as that of soft tissue, approximately 1540 m/s [17]. The phantom mixture was also enriched with 1% cellulose to simulate the acoustic backscattering of breast parenchymal tissue [17]. The phantom was constructed by suspending the vessel in an acrylic box and pouring the molten agar mixture around it.

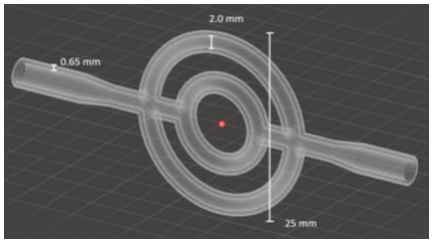

FIG 2. Computer-aided design (CAD) illustration of the 3D printed vessel embedded in the flow phantom. The outer diameter of the overall structure is 25 mm, the vessel inner diameter is 2 mm, and the vessel wall thickness is 0.65 mm.

A second, wall-less, phantom was created by placing silicon vasculature (Fig. 3) into an acrylic mold. The vasculature was cast using silicon rubber (Mold Star, Macungie, PA) into 3D-printed negative molds to make two vessel networks. Branches of the negative mold were aligned with 20-gauge galvanized steel wire (BEN-MOR, St-Hyacinthe, QC) before pouring the silicon mixture to act as a skeleton. The diameter of either end of the vasculature was 10 mm, which narrowed to 3 mm in the middle. The vessel networks were inserted into the acrylic mold through the inlet and outlet. They were then joined inside the acrylic mold by inserting branches from one network into holes at the end of the second network's branches. Molten agar was then poured into the mold and allowed to harden before the two halves of the vasculature were pulled out, creating wall-less channels.

FIG 3. Image of silicon vasculature used to create the wall-less phantom. Diameters on either end of the vasculature are 10 mm, which narrows to 3 mm in the middle where the two halves join.

C. Doppler Signal Quantification

To simulate blood flow during the 3D scan, a blood-mimicking fluid (BMF) (Shelley Medical Imaging

Technologies, London, Ontario, Canada) was pumped through the phantom [18]. Flow rates of 14.1 cm/s and 30.5 cm/s were used for SMI and PD images of the vessel mimic phantom, respectively. A flow rate of 6.5 cm/s was used for the wall-less phantom for both PD and SMI images. During the scan, the transducer collected a series of 2D PD and SMI images as it was translated across the phantom, which were reconstructed into a 3D Doppler (or SMI) image as the 2D images were acquired.

Images of the vessel mimic phantom were visually inspected to ensure full saturation of the Doppler signal within the channels. The 3D Doppler images of the wall-less phantom were evaluated through a comparison of vessel lengths with contrast-enhanced computed tomography (CT) images. For CT imaging, the phantom was filled with water and an 8% concentration of Iohexol CT contrast agent (Omnipaque 350 mg/mL, GE Healthcare, United States). Vessels in the 3D Doppler and CT images were segmented, and the vessel centerlines were extracted using 3D Slicer (3D Slicer, Boston, Massachusetts, Version 5.2.2). Centerline lengths were compared across 3D PD, 3D SMI, and CT images.

III. Results and Discussion

In addition to the design and fabrication of a novel 3D Doppler phantom, the proof-of-concept 3D Doppler ABUS images of the flow phantom are shown in Figs. 4 and 5. These results demonstrate the feasibility of 3D Doppler imaging using the 3D ABUS system. Importantly, this proof-of-concept demonstrates the ability of the ABUS system to reconstruct 3D images using both PD and SMI Doppler ultrasound, which is a capability not available with commercial systems. Figure 4 demonstrates the flow of fluid through the vessel mimic as its vessel channels are fully saturated with Doppler signal. The 3D Doppler images of the vessel mimic are also able to be dynamically viewed at any oblique and non-oblique views, such as coronal, transverse, and non-oblique visualization angles.

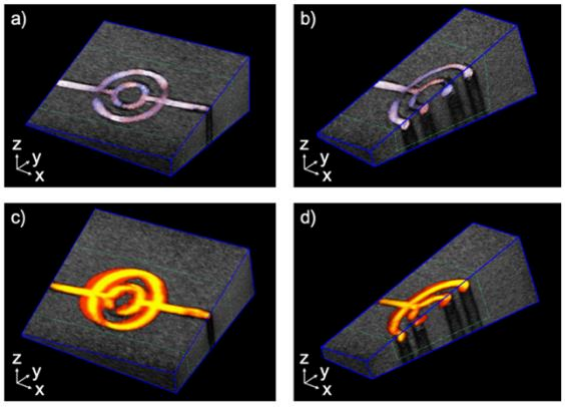

Fig 4. 3D Doppler ABUS images of the vessel mimicking phantom consisting of a 3D-printed vessel embedded in an agar gel. The top row shows a) coronal and b) transverse views of the vessel with SMI signal while the bottom row shows c) coronal and d) transverse views of the vessel with PD signal. The x, y, and z axes correspond to out-of-plane, in-plane, and elevational directions.

Figure 5 shows the segmented vessels in the wall-less phantom from the 3D PD and SMI images registered and overlapped with the CT images. These images show the saturation of the vessel branches by the Doppler signal. Vessel lengths in CT, PD, and SMI images were 428.54 mm, 450.24 mm, and 446.73 mm, respectively. Overall, vessel lengths were within 5% of each other. The mean distance between vessels from CT and 3D US images was 0.78 ± 0.5 mm.

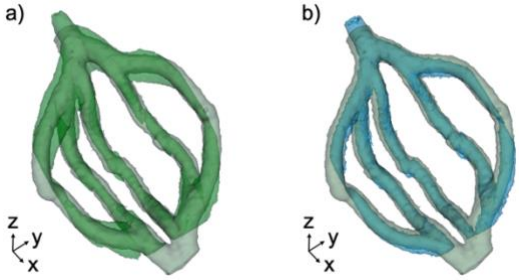

Fig 5. Coronal view of overlapping vessel segmentations for a) CT and PD images, and b) CT and SMI images of the wall-less phantom. The x, y, and z axes correspond to out-of-plane, in-plane, and elevational directions, respectively.

VI. Conclusion

We successfully developed an automated, cost-effective, portable, and patient-dedicated 3D ABUS system capable of 3D PD and SMI imaging, which marks the first whole-breast 3D Doppler image acquisition and generation using any commercially available US system and transducer equipped with Doppler capabilities. This addresses a critical gap in current ABUS technology and expands its diagnostic utility beyond conventional B-mode imaging. These results demonstrate the potential to improve the characterization of breast cancers, especially in increased-risk populations, including those with dense breasts. The improved characterization capabilities would allow for earlier detection, diagnosis, and overall increase in the likelihood of survival in populations impacted with breast cancer. Future studies will include 3D ABUS imaging of flow phantoms with disorganized and chaotic blood flow patterns as well as healthy volunteer and patient imaging.

Acknowledgements

This research was supported by the Canadian Institute for Health Research (CIHR), the Natural Sciences and Engineering Research Council (NSERC) of

Canada, and the Ontario Institute for Cancer Research (OICR) Imaging Program.

CONFLICT OF INTEREST

The authors declare they have no conflicts of interest.

REFERENCES

[1] M. Arnold *et al.*, "Current and future burden of breast cancer: Global statistics for 2020 and 2040," *Breast Off. J. Eur. Soc. Mastology*, vol. 66, pp. 15–23, Sep. 2022, doi: 10.1016/j.breast.2022.08.010.

[2] R. Burton and R. Bell, "The Global Challenge of Reducing Breast Cancer Mortality," *The Oncologist*, vol. 18, no. 11, pp. 1200–1202, Nov. 2013, doi: 10.1634/theoncologist.2013-0315.

[3] I. Leconte *et al.*, "Mammography and Subsequent Whole-Breast Sonography of Nonpalpable Breast Cancers: The Importance of Radiologic Breast Density," *Am. J. Roentgenol.*, vol. 180, no. 6, pp. 1675–1679, Jun. 2003, doi: 10.2214/ajr.180.6.1801675.

[4] N. F. Boyd *et al.*, "Mammographic Density and the Risk and Detection of Breast Cancer," *N. Engl. J. Med.*, vol. 356, no. 3, pp. 227–236, Jan. 2007, doi: 10.1056/NEJMoa062790.

[5] W. A. Berg, "Current Status of Supplemental Screening in Dense Breasts," *J. Clin. Oncol. Off. J. Am. Soc. Clin. Oncol.*, vol. 34, no. 16, pp. 1840–1843, Jun. 2016, doi: 10.1200/JCO.2015.65.8674.

[6] A. Cochet *et al.*, "Evaluation of breast tumor blood flow with dynamic first-pass 18F-FDG PET/CT: comparison with angiogenesis markers and prognostic factors," *J. Nucl. Med. Off. Publ. Soc. Nucl. Med.*, vol. 53, no. 4, pp. 512–520, Apr. 2012, doi: 10.2967/jnumed.111.096834.

[7] P. Busilacchi, F. Draghi, L. Preda, and C. Ferranti, "Has color Doppler a role in the evaluation of mammary lesions?," *J. Ultrasound*, vol. 15, no. 2, pp. 93–98, Jun. 2012, doi: 10.1016/j.jus.2012.02.007.

[8] D. S. Babcock, H. Patriquin, M. LaFortune, and M. Dauzat, "Power doppler sonography: basic principles and clinical applications in children," *Pediatr. Radiol.*, vol. 26, no. 2, pp. 109–115, 1996, doi: 10.1007/BF01372087.

[9] S. Artul, W. Nseir, Z. Armaly, and M. Soudack, "Superb Microvascular Imaging: Added Value and Novel Applications," *J. Clin. Imaging Sci.*, vol. 7, p. 45, 2017, doi: 10.4103/jcis.JCIS_79_17.

[10] M. Keçeli, Z. Keskin, and S. Keskin, "Comparison of Superb Microvascular Imaging With Other Doppler Methods in Assessment of Testicular Vascularity in Cryptorchidism," *Ultrasound Q.*, vol. 36, no. 4, pp. 363–370, Dec. 2020, doi: 10.1097/RUQ.0000000000000533.

[11] S. H. Kim, H. H. Kim, and W. K. Moon, "Automated Breast Ultrasound Screening for Dense Breasts," *Korean J. Radiol.*, vol. 21, no. 1, pp. 15–24, Jan. 2020, doi: 10.3348/kjr.2019.0176.

[12] C. Park, "Development and Validation of Mechatronic Systems for Image-Guided Needle Interventions and Point-of-Care Breast Cancer Screening with Ultrasound (2D and 3D) and Positron Emission Mammography," *Electron. Thesis Diss. Repos.*, May 2023, [Online]. Available: https://ir.lib.uwo.ca/etd/9315

[13] Aaron Fenster, Jeffrey Bax, David Tessier, and Claire K S Park, "Wearable 3D ultrasound-based whole breast imaging system"

[14] C. Park, J. Bax, D. Tessier, L. Gardi, and A. Fenster, "Design of a patient-specific whole-breast 3D ultrasound device for point-of-care imaging," in *Sixty-Eighth Annual Scientific Meeting of Canadian Organization of Medical Physicists*, Quebec City, Montreal, Canada: Medical Physics, Aug. 2022, pp. 5696–5696. doi: https://doi.org/10.1002/mp.15896.

[15] C. K. S. Park *et al.*, "Improving three-dimensional automated breast ultrasound resolution with orthogonal images," in *Medical Imaging 2023: Ultrasonic Imaging and Tomography*, SPIE, Apr. 2023, pp. 8–14. doi: 10.1117/12.2653141.

[16] Aaron Fenster, Jeffrey Bax, David Tessier, Igor Gyacskov, Claire K S Park, and Tiana Trumpour, "System and method for oblique plane visualization in 3D ultrasound imaging," 63/447,512, Feb. 22, 2022

[17] D. W. Rickey, P. A. Picot, D. A. Christopher, and A. Fenster, "A wall-less vessel phantom for Doppler ultrasound studies," *Ultrasound Med. Biol.*, vol. 21, no. 9, pp. 1163–1176, Jan. 1995, doi: 10.1016/0301-5629(95)00044-5.

[18] K. V. Ramnarine, D. K. Nassiri, P. R. Hoskins, and J. Lubbers, "Validation of a new blood-mimicking fluid for use in Doppler flow test objects," *Ultrasound Med. Biol.*, vol. 24, no. 3, pp. 451–459, Mar. 1998, doi: 10.1016/s0301-5629(97)00277-9.